



## Original Research Paper

Effect of BaF<sub>2</sub> powder addition on the synthesis of YAG phosphor by mechanical methodKazuaki Kanai<sup>a,\*</sup>, Yoshifumi Fukui<sup>a</sup>, Takahiro Kozawa<sup>b</sup>, Akira Kondo<sup>b</sup>, Makio Naito<sup>b</sup><sup>a</sup> Kaneka Fundamental Technology Research Alliance Laboratories, Kaneka Corporation, 2-8 Yamadaoka, Suita, Osaka, 565-0871, Japan<sup>b</sup> Joining and Welding Research Institute, Osaka University, 11-1 Mihogaoka, Ibaraki, Osaka, 567-0047, Japan

## ARTICLE INFO

## Article history:

Received 30 April 2016

Received in revised form 12 July 2016

Accepted 14 July 2016

Available online 29 July 2016

## Keywords:

YAG:Ce<sup>3+</sup>

Phosphor

White light emitting diode

Attrition-type mill

Mechanical synthesis

BaF<sub>2</sub>

## ABSTRACT

Here, we report on the effect of BaF<sub>2</sub> powder addition on the mechanical synthesis of Ce<sup>3+</sup>-doped Y<sub>3</sub>Al<sub>5</sub>O<sub>12</sub> (Y<sub>2.97</sub>Al<sub>5</sub>O<sub>12</sub>:Ce<sub>0.03</sub>, YAG:Ce<sup>3+</sup>) phosphors for white light emitting diodes. The YAG phosphors were synthesized by the mechanical method using an attrition-type mill. When BaF<sub>2</sub> was added at 6 wt% to the raw powder materials and milled, the synthesis of YAG:Ce<sup>3+</sup> was favorably achieved at the vessel temperature of 255 °C, which was about 1200 °C lower than the YAG phosphor synthesis temperature by solid-state reaction. The synthesized YAG:Ce<sup>3+</sup> phosphor revealed the maximum internal quantum yield of 57%.

© 2016 The Society of Powder Technology Japan. Published by Elsevier B.V. and The Society of Powder Technology Japan. All rights reserved.

## 1. Introduction

White light emitting diodes (LEDs) have been attracted much attention because they promise excellent high brightness, compact size, low-power consumption and long lifetime. They are composed of a blue chip (InGaN) and Ce<sup>3+</sup>-doped Y<sub>3</sub>Al<sub>5</sub>O<sub>12</sub> (yttrium aluminum garnet, YAG) phosphor. When the electron transition of Ce<sup>3+</sup> ions from 5d state to the ground state 4f is done, YAG phosphor can be efficiently converted from blue light to yellow light due to the excitation by the blue chip [1]. Furthermore, the emission wavelength can be easily controlled by changing the crystal field of host materials [2,3]. Conventionally, YAG:Ce<sup>3+</sup> phosphor was prepared by solid-state reaction at high temperatures. The raw powders such as Y<sub>2</sub>O<sub>3</sub>, Al<sub>2</sub>O<sub>3</sub>, and CeO<sub>2</sub> were mixed by ball milling, and then the mixed powder was calcined for several hours over 1600 °C to obtain YAG:Ce<sup>3+</sup> [4]. To achieve more energy saving process and lower manufacturing cost, drastic decrease of the calcination temperature is very effective.

To decrease the synthetic temperature, the addition of BaF<sub>2</sub> as a flux has been reported [5,6]. A single phase YAG:Ce<sup>3+</sup> was obtained at 1500 °C. BaF<sub>2</sub> reacts with raw materials to form eutectic compositions with lower melting point, and the subsequent solid-liquid reaction proceeds to the formation of YAG:Ce<sup>3+</sup>. However, the phosphor synthesis needs multi-step processes including still high

temperature calcination, thus leads to high manufacturing cost with huge heating energy.

According to the previous reports, YAG powder synthesis has been attempted by using a planetary ball mill without extra-heat assistance. But the synthesis of high crystalline YAG has not been done by only the milling process [7,8]. It is still unclear the reason, but the small power (about 0.8 kW) applied to the planetary ball mill [8] may be insufficient for the synthesis. On the other hand, mechanical method has achieved the synthesis of many kinds of composite oxides such as LiCoO<sub>2</sub> [9], LiMnPO<sub>4</sub> [10], LiFePO<sub>4</sub> [11] and LiNi<sub>0.5</sub>Mn<sub>1.5</sub>O<sub>4</sub> [12] by applying an attrition-type mill without any extra-heat assistance. Therefore, if the synthesis of the YAG phosphor is achieved by using this approach, a new energy-saving and low-cost process will be developed.

In this paper, we focused on the direct synthesis of the YAG:Ce<sup>3+</sup> phosphor by applying attrition-type mill. The raw materials of YAG:Ce<sup>3+</sup> were processed with addition of BaF<sub>2</sub> by using attrition-type mill. BaF<sub>2</sub> was added for the purpose of the lower temperature synthesis of YAG:Ce<sup>3+</sup>. The fluorescent properties of the obtained YAG:Ce<sup>3+</sup> phosphors were then evaluated.

## 2. Experimental

## 2.1. Raw materials

Commercially available Y<sub>2</sub>O<sub>3</sub>, Al<sub>2</sub>O<sub>3</sub> and CeO<sub>2</sub> were used as raw materials. Micron size powder of BaF<sub>2</sub> was used as the raw material

\* Corresponding author.

E-mail address: [Kazuaki.Kanai@kaneka.co.jp](mailto:Kazuaki.Kanai@kaneka.co.jp) (K. Kanai).

of flux. These high-purity powders were purchased from Kojundo Chemical Laboratory (Japan). Some characteristics of these powders are summarized in Table 1. The median size ( $D_{50}$ ) of the raw powder was calculated by the particle size distribution, measured by the laser diffraction-scattering method (MICROTRAC MT3300EXII, NIKKISO, JAPAN). The specific surface area ( $S_w$ ) of raw powders was measured by a  $N_2$  adsorption instrument (MICROMERITICS ASAP2010, SHIMADZU, JAPAN) based on the BET method. The primary particle size ( $d_{BET}$ ) was calculated from the BET specific surface area by using the following equation:  $d_{BET} = 6/(\rho \cdot S_w)$ , where  $\rho$  is a theoretical density. The primary particle sizes of  $Y_2O_3$ ,  $Al_2O_3$ ,  $CeO_2$  and  $BaF_2$  were 72 nm, 134 nm, 5 nm and 137 nm, respectively.

## 2.2. Mechanical synthesis and solid-state reaction

In this study, we selected the chemical composition of  $Y_{2.97}Al_{5.03}O_{12}:Ce_{0.03}^{3+}$  as  $YAG:Ce^{3+}$ . Stoichiometric quantities of  $Y_2O_3$ ,  $Al_2O_3$ , and  $CeO_2$  were 16.90, 12.84 g and 0.26 g, respectively. Then the mixture (total amount of 30 g) was put into the vessel of the attrition-type mill. 4, 6 and 10 wt% of  $BaF_2$  for the weight of raw materials were selected to discuss the role of flux for the mechanical synthesis. The milling apparatus has been illustrated elsewhere [9]. The main parts of this mill are a fixed chamber (inner diameter of 80 mm, depth of 50 mm) and an oval rotor, which was made by a stainless steel. The gap between the chamber and the rotor was fixed at 1 mm. The powder processing by using this attrition-type mill was carried out while cooling the chamber wall by water. The milling was conducted at electric power of 3 kW for 10 min, where this electric power is defined as the load power applied to the motor shaft. For the sake of simplicity, the mixed powders obtained at  $BaF_2$  of 4, 6, and 10 wt% are denoted as sample A, B and C, respectively. In order to compare the solid-state reaction and the mechanical method, mixing of raw materials by conventional ball milling was also conducted. The same amount of raw materials with 6 wt%  $BaF_2$  was put into ethanol in a  $ZrO_2$  pot (inner diameter of 100 mm, depth of 120 mm) together with  $ZrO_2$  balls of 5 mm diameter. The ball milling was performed at a rotation speed of 60 rpm for 6 h. The ball milled powder is denoted as sample D. Then,  $YAG:Ce^{3+}$  phosphor was synthesized by solid-state reaction. Each mixed sample D was calcined at 1400 °C and 1500 °C for 3 h in a  $N_2$  atmosphere, respectively. After calcining, the synthesized  $YAG:Ce^{3+}$  products were pulverized to obtain powders. Then, the YAG phosphor powders were washed thoroughly with diluted hydrochloric acid and pure water to eliminate  $BaF_2$  in the powders and dried in an oven at 120 °C.

## 2.3. Characterization

The particle morphology and microstructure was observed by scanning electron microscopy (SEM, CARLZEISS, ULTRA PLUS). The crystalline phases of the  $YAG:Ce^{3+}$  products were identified by a powder X-ray diffraction measurement system (XRD, RIGAKU, ULTIMA IV).

The crystallite size ( $D_c$ ) was estimated from the Scherrer equation by using the following equation:  $D_c = 0.9\lambda/(\beta \cdot \cos\theta)$ , where  $\lambda$  is the employed X-ray wavelength,  $\theta$  is the diffraction angle, and  $\beta$  is defined as the half-width. Crystallite size was estimated by using (400) peak of YAG phase.

**Table 1**  
Powder properties of the starting materials used in this study.

Materials	Purity (%)	$D_{50}$ ( $\mu\text{m}$ )	$S_w$ ( $\text{m}^2/\text{g}$ )	$d_{BET}$ (nm)
$BaF_2$	99.99	2.6	9.0	137

The fluorescent properties of  $YAG:Ce^{3+}$  phosphors were evaluated by using the obtained powders. The photoluminescence (PL) properties were measured by a fluorescence spectrophotometer (HITACHI, F-7000). The internal quantum yield (QY) and absorptivity (Abs) were measured by a quantum yield measurement device (HAMAMATSU PHOTONICS QUANTAUROS-QY C11347-01).

## 3. Results and discussion

### 3.1. Mechanical synthesis of $YAG:Ce^{3+}$ phosphors

$YAG:Ce^{3+}$  phosphors were synthesized by mechanical method. Fig. 1 shows the XRD patterns of the products obtained from mechanical synthesis by using different content of  $BaF_2$ . The powders were processed by the attrition-type mill at electric power of 3 kW for 10 min. Fig. 1 shows that sample A (4 wt% of  $BaF_2$ ) has the diffraction peaks of almost raw material ( $Y_2O_3$  and  $Al_2O_3$ ) phases. However, in the sample B (6 wt% of  $BaF_2$ ), the diffraction peaks of YAG phase appeared, and they were almost same as those of sample C (10 wt% of  $BaF_2$ ). During the processing by the attrition-type mill, the maximum vessel temperature was kept 255 °C. The reduction of  $Ce^{+4}$  occurs in the range from 1300 °C to 1500 °C, where YAG is synthesized [4]. By mechanical method, the local temperature of particle surface reaches almost ten times higher than the vessel temperature (255 °C) [13]. Therefore, the reduction is thought to occur during the mechanical processing. It means that  $YAG:Ce^{3+}$  phase was successfully synthesized by only mechanical processing at low temperature without any extra-heat assistance.

### 3.2. Solid-state synthesis of $YAG:Ce^{3+}$ phosphors

$YAG:Ce^{3+}$  phosphors were synthesized by calcining sample D. Fig. 2 shows the XRD patterns of the products obtained from two samples D by calcining at different temperatures. When the mixed powder prepared by the ball milling was calcined at 1400 °C, the yttrium aluminum oxide and barium aluminate ( $YAlO_3$  and  $BaAl_2O_4$ ) were formed as an intermediate phase. However, the diffraction peaks of these intermediate phases decreased with elevated calcination temperature. As a result, the  $YAG:Ce^{3+}$  single phase was obtained at 1500 °C.

### 3.3. Microstructure of $YAG:Ce^{3+}$ phosphors by mechanical synthesis

Fig. 3 shows the SEM image of sample B, and Fig. 4(a) shows the SEM image of the cross section view of sample B. As shown in Fig. 3, the sample B was composed of granules.

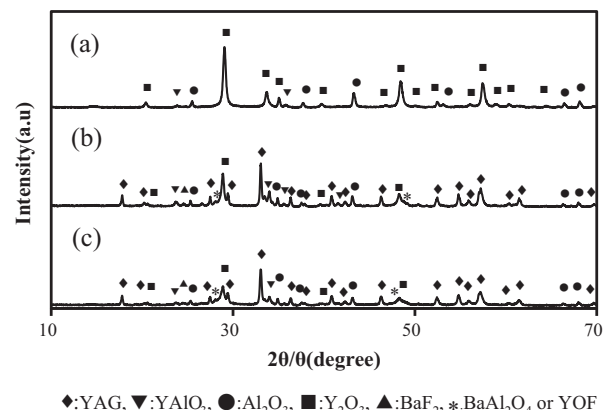


**Fig. 1.** XRD patterns of the products obtained by mechanical method of (a) sample A, (b) sample B and (c) sample C.

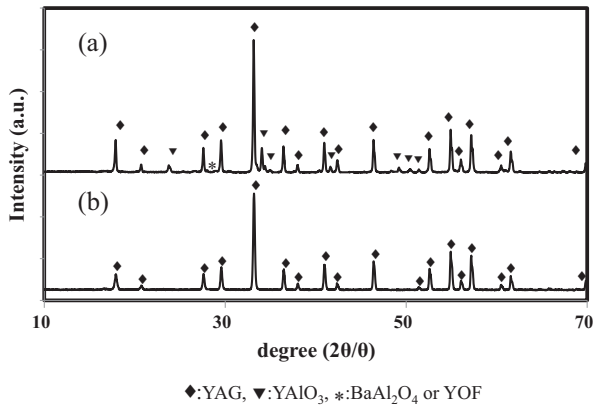
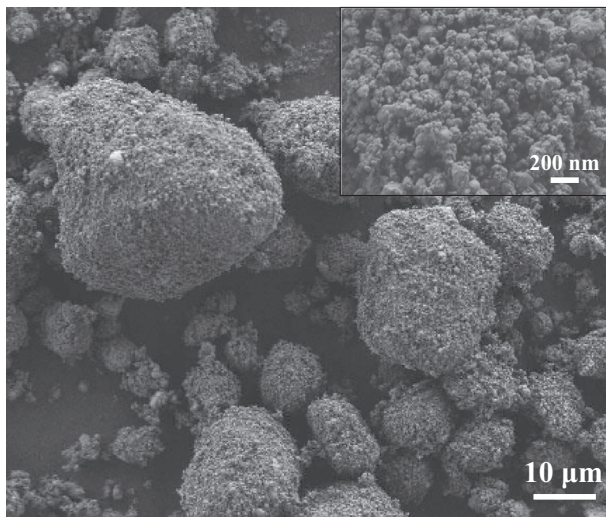


**Fig. 2.** XRD patterns of the products obtained by solid state reaction of sample D: (a) calcined at 1400 °C, (b) 1500 °C.

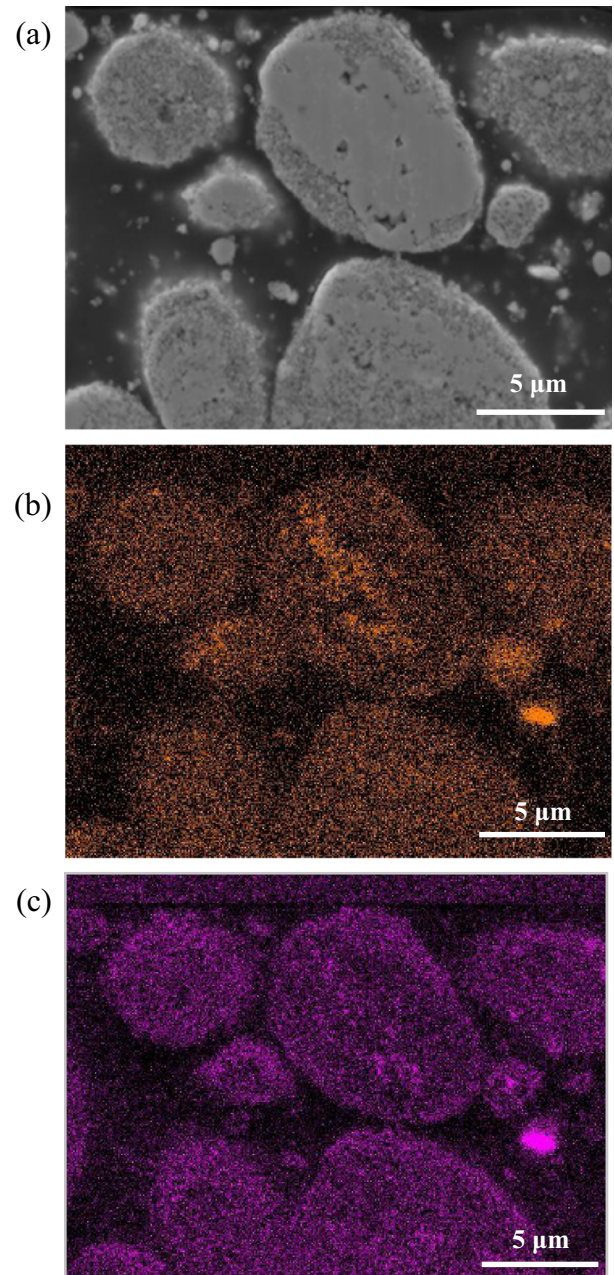
The surface of the granule at high magnification as shown in the inset of Fig. 1 shows that the surface is composed of fine particles. However, densely packed structure is observed inside of the granules although the surface structure forms fine particles layer as shown in Fig. 4(a). Fig. 4(b) shows the EDX map of Ba (orange) and Fig. 4(c) shows that of F (purple). Both figures indicate that both elements are dispersed uniformly inside of granules, although some parts are observed as BaF<sub>2</sub> agglomerates.

Fig. 5(a) shows the SEM images of the cross section view of densely packed structure of the granule in sample B. It is observed that very fine particles are dispersed inside of the sintered structure as indicated by arrows. The size of fine particles is almost consistent with the primary particle size ( $d_{\text{BET}}$ ) of BaF<sub>2</sub>. On the other hand, Fig. 5(b) and (c) shows the EDX maps of Ba and F, respectively. Both maps show that fine particles of BaF<sub>2</sub> are apparently dispersed in the sintered structure.

Higher magnification image of the cross section as shown in the inset of Fig. 5(a) suggests that particles sinter each other and form YAG:Ce<sup>3+</sup> phosphor. It is supposed that BaF<sub>2</sub> was finely dispersed in the granule by the mechanical processing, and then contributed to the synthesis of YAG:Ce<sup>3+</sup> phosphor through the liquid-solid reaction at lower temperature [5,6]. Nogi et al reported that the local temperature of particle surface reaches about ten times higher than the average temperature of the powder processed by mechan-



**Fig. 3.** SEM image of sample B.

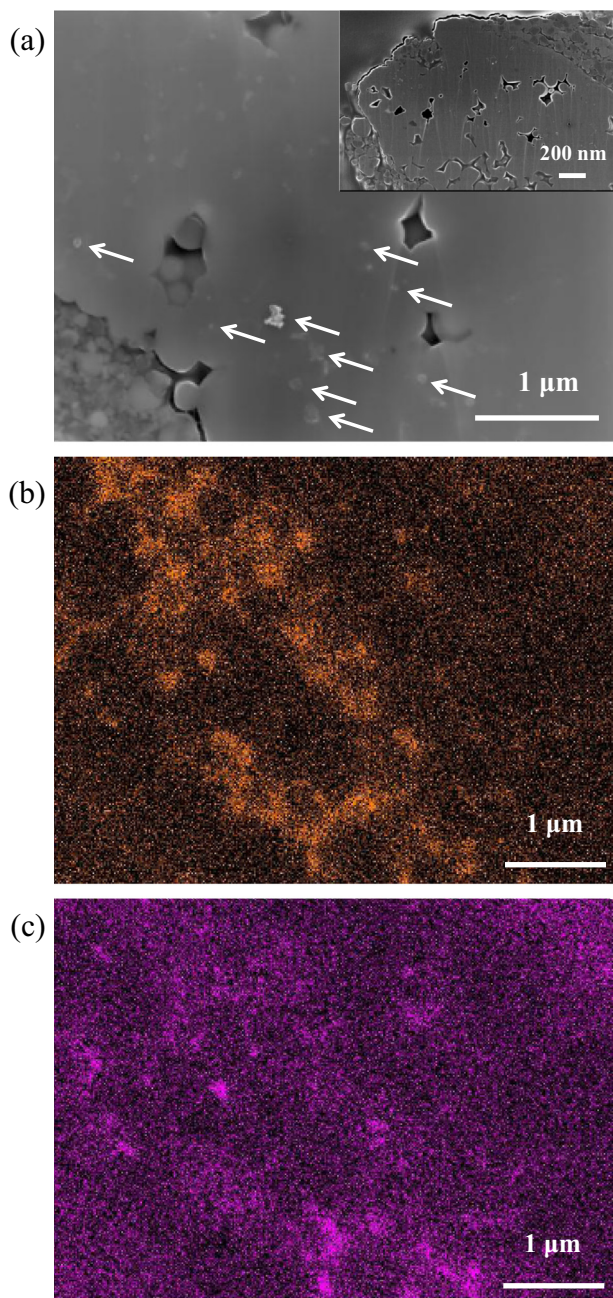


**Fig. 4.** Cross section views of sample B: (a) SEM image, (b) EDX elemental map of Ba (orange), (c) F element (purple). (For interpretation of the references to colour in this figure legend, the reader is referred to the web version of this article.)

ical method [13]. The synthesis of YAG:Ce<sup>3+</sup> phosphor is done with BaF<sub>2</sub> at 1500 °C [5,6]. On the other hand, the maximum temperature of the vessel during the milling reached 255 °C. Therefore, it is discussed that fine particle of BaF<sub>2</sub> can be easily melted by the mechanical method, thus led to the solid liquid phase reaction. As a result, it is concluded that YAG phase is easily obtained without any extra-heat assistance.

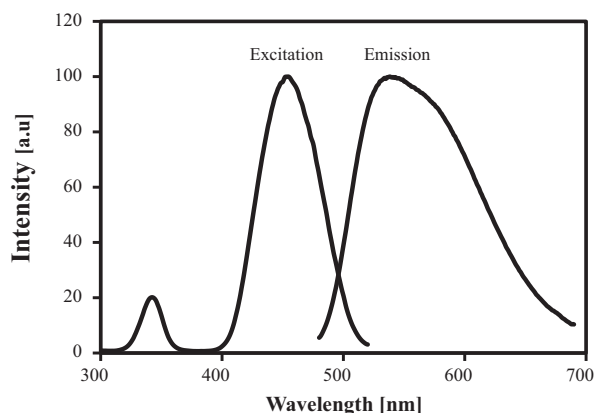
### 3.4. Fluorescence property

Fig. 6 shows an example of the photoluminescence (PL) spectra of YAG:Ce<sup>3+</sup> phosphors prepared from sample B. The peak of excitation wavelength (Ex) was 460 nm and the peak of the emission spectrum (Em) was 540 nm.



**Fig. 5.** Cross section views of densely packed structure of the granule in sample B. (a) SEM image, (b) EDX elemental map of Ba (orange), (c) F element (purple). (For interpretation of the references to colour in this figure legend, the reader is referred to the web version of this article.)

Table 2 shows the internal quantum yield (QY) and absorption (Abs) of synthesized  $\text{YAG:Ce}^{3+}$  phosphors which were measured at Ex = 460 nm and Em = 540 nm. The QY of 57% was obtained from sample B. However, both QY and Abs of sample B were lower than those obtained by the sample D calcined at 1500 °C. Table 2 also shows the crystallite size of sample B and sample C. The crystallite size was calculated by the Scherrer equation. The crystallite size decreased a little with the increase of  $\text{BaF}_2$  amount in the case of mechanical processing. It is reported the QY of  $\text{YAG:Ce}^{3+}$  phosphors increases with the increase of crystallite size [14]. It may be the reason why the QY of sample B was a little bit higher than that of sample C. On the other hand, the crystallite size of sample D calcined at 1500 °C was apparently larger than those of the mechan-



**Fig. 6.** Excitation and emission spectra of YAG phosphor of sample B.

**Table 2**

Internal quantum yield (QY), absorption (Abs) and crystallite size ( $D_c$ ) of samples.

Sample	QY (%)	Abs (%)	$D_c$ (nm)	$\text{BaF}_2$ (wt%)
B	57	45	39	6
C	55	34	37	10
D (calcined at 1500 °C)	75	63	47	6

Ex = 460 nm, Em = 540 nm.

ically processed samples. It suggests that the synthesis of  $\text{YAG:Ce}^{3+}$  phosphor with larger crystallite size is important for exhibiting a more favorable fluorescent property of mechanically processed samples.

As shown in Table 2, the Abs of mechanically processed samples are lower than that of sample D processed by solid-state reaction. It is still unclear the reason, but the surface roughness of particles may decrease the Abs [15]. Further analysis including the detail observation of the microstructure of the samples must be done for improving the Abs and QY as future works.

#### 4. Conclusions

- (1) The YAG phosphors were successfully synthesized by the mechanical method using an attrition-type mill with the addition of  $\text{BaF}_2$  as a flux. The  $\text{YAG:Ce}^{3+}$  phase was obtained at the maximum vessel temperature of 255 °C. It was about 1200 °C lower than the synthesis temperature by solid-state-reaction of the ball milled sample.
- (2) The  $\text{BaF}_2$  was effective for the liquid-solid phase reaction of YAG phosphor at lower temperature, thus led to the synthesis of YAG phosphor at the interface between particles during the mechanical processing without any extra-heat assistance.
- (3) The YAG phosphor obtained by mechanical method revealed the maximum internal quantum yield of 57% in the case of the sample processed at 6 wt% addition of  $\text{BaF}_2$ .

#### References

- [1] G. Blasse, A. Bril, Investigation of some  $\text{Ce}^{3+}$ -activated phosphors, *J. Chem. Phys.* 47 (1967) 5139–5145.
- [2] W.W. Holloway Jr., M. Kestigian, Optical properties of cerium-activated garnet crystals, *J. Opt. Soc. Am.* 59 (1969) 60–63.
- [3] M.C. Maniquiz, K.Y. Jung, S.M. Jeong, Luminescence characteristics of  $\text{Y}_3\text{Al}_5\text{-}_2\text{y}(\text{Mg, Si})_3\text{O}_{12}:\text{Ce}$  phosphor prepared by spray pyrolysis, *J. Electrochem. Soc.* 157 (2010) 1135–1139.

- [4] A. Ikesue, T. Kinoshita, Fabrication and optical properties of high-performance polycrystalline Nd:YAG ceramics for solid-state lasers, *J. Am. Ceram. Soc.* 78 (1995) 1033–1040.
- [5] K. Ohno, T. Abe, Effect of BaF<sub>2</sub> on the synthesis of the single-phase cubic Y<sub>3</sub>Al<sub>5</sub>O<sub>12</sub>:Tb, *J. Electrochem. Soc.* 133 (1986) 638–643.
- [6] K. Ohno, T. Abe, The synthesis and particle growth mechanism of bright green phosphor YAG:Tb, *J. Electrochem. Soc.* 141 (1994) 1252–1254.
- [7] X. Guo, K. Sakurai, Formation of yttrium aluminum perovskite and yttrium aluminum garnet by mechanical solid-state reaction, *Jpn. J. Appl. Phys.* 39 (2000) 1230–1234.
- [8] Q. Zhang, F. Saito, Mechanochemical solid reaction of yttrium oxide with alumina leading to the synthesis of yttrium aluminum garnet, *Powder Technol.* 129 (2003) 86–91.
- [9] E. Nakamura, A. Kondo, T. Kozawa, M. Naito, J. Yoshida, S. Nakanishi, H. Iba, One-pot mechanical synthesis of LiCoO<sub>2</sub> from Li<sub>2</sub>O powder, *J. Soc. Powder Technol. Jpn.* 51 (2014) 131–135.
- [10] J. Yoshida, S. Nakanishi, H. Iba, A. Kondo, H. Abe, M. Naito, One-step mechanical synthesis of the nanocomposite granule of LiMnPO<sub>4</sub> nanoparticles and carbon, *Adv. Powder Technol.* 24 (2013) 829–832.
- [11] T. Kozawa, N. Kataoka, A. Kondo, E. Nakamura, H. Abe, M. Naito, One-step mechanical synthesis of LiFePO<sub>4</sub>/C composite granule under ambient atmosphere, *Ceram. Int.* 40 (2014) 16127–16131.
- [12] T. Kozawa, A. Kondo, E. Nakamura, H. Abe, M. Naito, H. Koga, S. Nakanishi, H. Iba, Rapid synthesis of LiNi<sub>0.5</sub>Mn<sub>1.5</sub>O<sub>4</sub> by mechanical process and post-annealing, *Mater. Lett.* 132 (2014) 218–220.
- [13] K. Nogi, M. Naito, A. Kondo, A. Nakahira, K. Niihara, T. Yokoyama, New method for elucidation of temperature at the interface between particles under mechanical stirring, *J. Jpn. Soc. Powder Powder Metall.* 43 (1996) 396–401.
- [14] A. Purwanto, W. Ni. Wang, I.W. Lenggono, K. Okuyama, Formation and luminescence enhancement of agglomerate-free YAG:Ce<sup>3+</sup> submicrometer particles by flame-assisted spray pyrolysis, *J. Electrochem. Soc.* 154 (2007) J91–J96.
- [15] C.H. Chiang, T.H. Liu, H.Y. Lin, H.Y. Kuo, S.Y. Chu, Effects of flux additives on the characteristics of Y<sub>2.95</sub>Al<sub>5</sub>O<sub>12:0.05</sub>Ce<sup>3+</sup> phosphor: particle growth mechanism and luminescence, *J. Appl. Phys.* 114 (2013) (pp. 24517–1).